



Allogeneic CAR T Cells Targeting DLL3 Are Efficacious and Safe in Preclinical Models of Small Cell Lung Cancer

Yi Zhang¹, Silvia K. Tacheva-Grigorova¹, Janette Sutton¹, Zea Melton¹, Yvonne S.L. Mak¹, Cecilia Lay¹, Bryan A. Smith¹, Tao Sai², Thomas Van Blarcom¹, Barbra J. Sasu¹, and Siler H. Panowski¹

ABSTRACT

Purpose: Small cell lung cancer (SCLC) is an aggressive disease with limited treatment options. Delta-like ligand 3 (DLL3) is highly expressed on SCLC and several other types of neuroendocrine cancers, with limited normal tissue RNA expression in brain, pituitary, and testis, making it a promising CAR T-cell target for SCLC and other solid tumor indications.

Experimental Design: A large panel of anti-DLL3 scFv-based CARs were characterized for both *in vitro* and *in vivo* activity. To understand the potential for pituitary and brain toxicity, subcutaneous or intracranial tumors expressing DLL3 were implanted in mice and treated with mouse cross-reactive DLL3 CAR T cells.

Results: A subset of CARs demonstrated high sensitivity for targets with low DLL3 density and long-term killing potential *in vitro*. Infusion of DLL3 CAR T cells led to robust antitumor efficacy, including complete responses, in subcutaneous and systemic SCLC *in vivo* models. CAR T-cell infiltration into intermediate and posterior pituitary was detected, but no tissue damage in brain or pituitary was observed, and the hormone-secretion function of the pituitary was not ablated.

Conclusions: In summary, the preclinical efficacy and safety data presented here support further evaluation of DLL3 CAR T cells as potential clinical candidates for the treatment of SCLC.

Introduction

Small cell lung cancer (SCLC) is an aggressive neuroendocrine cancer with a high unmet medical need. This disease afflicts approximately 30,000 patients per year in the United States and carries an approximate 5-year overall survival rate of 5% (1). Because SCLC is commonly metastatic at the time of diagnosis, patients rarely benefit from surgery. Responses to chemotherapy and radiation are typically transient and almost all patients relapse. The recent addition of immune checkpoint blockade to first-line chemotherapy has shown modest treatment effects and changed the treatment landscape for SCLC (2–4) but a therapy that can substantially boost clinical outcome is still needed.

Adoptive transfer of T cells expressing chimeric antigen receptors (CAR) is a promising new therapy for hematologic malignancies, including recently approved CD19- and BCMA-targeting CAR T-cell therapies (5–9). These approved autologous CAR T therapies, while showing benefits for patients, still face multiple challenges, including time required for production and testing, complex supply chain logistics, variability in potency of patient-derived T cells and the need for a GMP process for each patient. Allogeneic CAR T cell therapy or “off-the-shelf” CAR T therapy that utilizes T cells from healthy donors may greatly reduce the time between patient enrollment and treatment and may also increase product activity and consistency (10, 11). To create an allogeneic product that does not elicit graft versus host disease (GvHD), CAR T cells in the current work have been genetically modified using Transcriptional Activator-Like Effector Nuclease (TALEN) gene-editing at the TRAC

locus to remove T-cell receptor complex from the cell surface. To lengthen the window of T-cell engraftment, the CAR T cells were further genetically modified using TALEN to remove CD52 to confer resistance to ALLO-647, an anti-CD52 antibody. This antibody can then be used as part of the lymphodepletion regimen for transient depletion of host immune cells to provide a niche for CAR T-cell expansion. Allogeneic CAR T cells using these edits and ALLO-647 are being evaluated clinically in lymphoma (ALLO-501/501A targeting CD19), multiple myeloma (ALLO-715/605 targeting BCMA), and renal cell carcinoma (ALLO-316 targeting CD70).

To identify potential CAR T-cell targets for SCLC, we analyzed public gene expression data and identified delta-like ligand 3 (DLL3) as a target with high expression in SCLC and low expression in normal tissues. DLL3 is one of the mammalian Notch family ligands that is expressed during embryonic development (12, 13). Unlike other Notch ligands that activate Notch receptor in trans, DLL3 is reported to inhibit Notch pathway activation by sequestering Notch receptor and ligands in intracellular compartments (14, 15). The Notch pathway was shown to be tumor-suppressive in neuroendocrine tumors (16–18) and may support SCLC tumor development by inhibiting Notch activation. However, Notch signaling was also shown to contribute to heterogeneity and play a protumorigenic role in SCLC, thus further work is needed to fully understand the role of DLL3 in SCLC (19, 20).

A DLL3-targeted antibody–drug conjugate (ADC) has previously been tested in the clinic and initially showed evidence of clinical activity (21) with no target-related toxicity, but demonstrated no clinical benefit in subsequent trials (22, 23) potentially due to the low density of DLL3 on the cell surface and limitations in dose escalation due to payload-related toxicities, rendering it a difficult target for ADC technology (24–26). For this reason, therapeutic agents against DLL3 which work well in lower target ranges may be of benefit for patients with SCLC. Previous studies have reported the use of DLL3-targeted Bispecific T-cell engager (BiTE), additional bi- and trispesific formats, and CAR NK cells in SCLC preclinical models (27–31), all of which are currently in the clinic. Our study is the first to characterize a DLL3 CAR T program utilizing a large number of single chain variable fragment (scFv)-based anti-DLL3 CAR T-cell clones and identify potential clinical candidates. Here, we demonstrate that DLL3 CAR T cells

¹Allogene Therapeutics, South San Francisco, California. ²Pfizer Worldwide Research and Development, South San Francisco, California.

Corresponding Authors: Siler H. Panowski, Research, Allogene Therapeutics, Inc., 210 East Grand Avenue, South San Francisco, CA, 94080. E-mail: siler.panowski@allogene.com; and Barbra J. Sasu, barbra.sasu@allogene.com
Clin Cancer Res 2023;XX:XX–XX

doi: 10.1158/1078-0432.CCR-22-2293

©2023 American Association for Cancer Research

Translational Relevance

Small cell lung cancer (SCLC) is an aggressive neuroendocrine malignancy with a poor prognosis and high need for new therapies. A therapeutic approach that has demonstrated substantial benefit in hematologic malignancies is the adoptive transfer of T cells expressing chimeric antigen receptors (CAR). The clinical benefit of CARs in solid tumor indications has been limited, in part due to the lack of suitable tumor-associated antigens. This study identifies and validates DLL3 as an attractive tumor-associated antigen for the treatment of SCLC with CAR T cells. A large panel of DLL3 CAR T cells was extensively evaluated both *in vitro* and *in vivo* to identify an anti-DLL3 CAR T candidate that was highly efficacious and maintained an acceptable safety profile in complex mouse safety models. Taken together, these results suggest that anti-DLL3 CAR T cells may provide meaningful clinical benefit to patients with SCLC.

have potent and specific activity against SCLC cell lines *in vitro*, including high sensitivity for cells with very low levels of antigen density (<1,000 DLL3 molecules per cell and similar to the range of DLL3 expression expected on primary tumors). We also demonstrate that a single injection of DLL3 CAR T cells leads to significant tumor control, including complete antitumor responses, in multiple SCLC subcutaneous and systemic models. Despite low levels of *DLL3* RNA expression in pituitary and brain, DLL3 CAR T cells were well tolerated in mouse safety studies. T-cell infiltration in pituitary was observed but no tissue damage was found. The potent activity of DLL3 CAR T cells in SCLC models, the favorable preclinical safety profiles, together with the promise of allogeneic CAR T cell therapy, support the clinical investigation of allogeneic DLL3 CAR T-cell for the treatment SCLC.

Materials and Methods

Study design

DLL3 expression on SCLC cell lines, primary tumors, patient-derived xenograft (PDX) models, and normal tissues was assessed using RNA *in situ* hybridization, flow cytometry, or IHC. DLL3 mAbs were generated by immunizing animals with recombinant DLL3 proteins and binding kinetics and epitopes were determined. DLL3 CAR T cells were generated from multiple human T-cell donors and *in vitro* functional assays (including various cytotoxicity assays and cytokine secretion) were performed with three to six replicates. All animal studies were performed under approval by the Allogene Therapeutics Institutional Animal Care and Use Committee (IACUC) using 7- to 9-week-old female NOD.Cg-Prkdc^{scid} Il2rg^{tm1Wjl}/SzJ (NSG) mice from The Jackson Laboratory. Animals were housed under ambient conditions, with free access to water and standard rodent chow. Animals were euthanized when they exhibited disease model-specific endpoints. *In vivo* studies with subcutaneous or systemic SCLC models were performed with $n = 8$ to 10 mice per group of NSG mice. A tissue cross reactivity (TCR) assay was performed to assess off-target binding of CAR scFvs against a panel of 36 normal tissues. One of the lead CARs showed pancreatic membrane staining and this was considered a potential safety liability. To further assess this staining, a follow-up study was performed using pancreas samples from an additional eight human donors. Binding and T-cell activation assay were also performed using primary pancreatic cells from 3

human donors to confirm no direct binding of or T-cell activation by primary cells. To evaluate potential on-target toxicity in brain and pituitary, we evaluated T-cell infiltration and tissue damage in NSG mice bearing subcutaneous or intracranial tumors, because activation of CAR T cells by tumor cells may lead to increased activity against potential DLL3-expressing normal tissue.

Cell lines

SHP-77, WM266-4, DMS454, and DMS273 are DLL3 positive lines that were purchased from ATCC or Sigma. No authentication was performed, and all cells were purchased directly from the source. No misidentified cell lines were used. DMS273-DLL3 were generated by transducing DMS273 with lentivirus encoding full length human *DLL3* to increase DLL3 surface copy number. LN229 cells expressing mouse DLL3 (LN229-mDLL3) were generated by transducing LN229 with lentivirus encoding full-length mouse *DLL3* to understand on-target toxicity in mouse models. DMS273 and WM266-4 cells expressing nuclear GFP were generated by transducing cells with Nuclight Green Lentivirus (Satorius) and used in incucyte kinetic killing assay. For *in vivo* and *in vitro* bioluminescent analysis, luciferin-expressing versions of all cell lines were generated by transducing with lentivirus encoding Luc2-GFP. Early passages of cells were frozen down and prior to initiating experiments cells were thawed and passaged two to three times. All cell lines were tested for mycoplasma and were negative.

Staining and quantification of DLL3 by flow cytometry

Disassociated SCLC PDX cells were obtained from Crown Bioscience. SCLC cell lines and PDX cells were stained with 10 µg/mL of anti-DLL3 antibody conjugated to phycoerythrin (PE) at a 1:1 ratio. Antibody binding capacity was quantified using Quantibrite PE beads (BD Biosciences) following manufacturer's protocol. Samples were acquired on CytoFLEX flow cytometer (Beckman Coulter).

Antibody development

Recombinant Flag-DLL3 (Adipogen) or DLL3(EGF1-EGF6)-Avi-His protein purified in-house from supernatants of transfected Expi293 cells was used as an immunogen. Hybridomas were generated from mice and rats expressing functional human Ig genes (Alivamab mouse and OmniRat). Anti-DLL3 antibodies were first screened using a Flag-DLL3 (Adipogen) ELISA and then confirmed to target cellular DLL3 by flow cytometry against HEK-293T cells with or without human DLL3 expression. The antibodies were further counter-screened against structurally similar Notch ligands DLL1, DLL4, Jagged-1, and Jagged-2 (R&D systems) using ELISA.

DLL3 CAR T production

HEK293T cells were transfected with the CAR construct along with psPAX2 and pMD.2G plasmids at a ratio of 1:3:1, respectively, using Lipofectamine2000 (Invitrogen) according to the manufacturer's protocol to produce lentivirus supernatant. Primary T cells were activated using human TransAct (Miltenyi) using manufacturer's protocol and 2 days later transduced with 50% LVV supernatant (v/v) and then cultured in X-Vivo 15 medium supplemented with 5% human AB serum (Gemini Bio-Products). Where T-cell receptor- α (TRAC) and CD52 knockout T cells were used, 6 days after activation T cells were electroporated with TALEN mRNA (Collectis & TriLink Biotechnologies) as described previously (23). Cells were stained on day 9 post-activation with anti-CD25, and anti-4-1BB, and on Day 14 with anti-CD62 L and anti-CD45RO. Recombinant human IL2 (Miltenyi) was added throughout T-cell culture at 100IU/mL every 2 to 3 days and

TCR $\alpha\beta$ -positive cells were depleted using Human TCR Alpha/Beta Depletion Kit (StemCell Technologies) by the end of process. T cells were cryopreserved in 90% FBS/10% DMSO and all functional assays were performed with cells after recovery from cryopreservation.

***In vitro* cytotoxicity and cytokine secretion**

To perform short-term cytotoxicity assay, DLL3 CAR T cells were incubated with luciferase-labeled SHP-77, WM266-4, DMS454, or DMS273 cells at defined effector:target (E:T) ratios. Target viability was measured after 72 hours using ONE-Glo Assay Kit (Promega). To perform long-term serial killing assay, target cells and CAR T cells were co-cultured as described above. Every 2 to 3 days thereafter, two thirds of the medium (100 μ L) containing DLL3 CAR T cells were transferred to freshly plated target cells. Target cell viability in the spent plate was read out using ONE-Glo Assay Kit. Each condition was assayed in three to six replicates. To detect cytokine secretion, DLL3 CAR T cells were incubated with target cells at E:T ratio of 1:1 in 96-well plates. Twenty-four hours later, tissue culture supernatant was collected and the levels of cytokines in the supernatants were measured using human proinflammatory tissue culture 9-plex assay (MSD) following manufacturer's protocol.

***In vivo* activity in subcutaneous and systemic models**

All animal studies were performed under approval by the Allogene Therapeutics Institutional Animal Care and Use Committee (IACUC). For subcutaneous models, SHP-77 cells (5×10^6 per mouse) or DMS273-DLL3 cells (1×10^5 per mouse) were injected in 200 μ L subcutaneously 1:1 with Matrigel Membrane Matrix (Corning 354234) in NSG mice. Tumor growth was monitored by caliper measurements and tumor size was calculated using the formula Tumor volume = (width² \times length)/2. Two weeks postimplantation mice were assigned to groups such that each group had similar mean \pm SD tumor volume. CAR T cells were injected intravenously (5×10^6 CAR⁺ cells/mouse in the SHP-77 model or 1×10^7 CAR⁺ cells/mouse in the DMS273-DLL3 model). Tumor measurements were taken every 3 to 4 days until the end of the study.

For systemic models, luciferase-labeled SHP-77 cells (1×10^6 per mouse) or DMS273-DLL3 cells (1×10^5 per mouse) were injected in 200 μ L intravenously in NSG mice. Tumor growth was monitored by bioluminescence imaging (BLI). Mice were assigned to groups such that each group had similar mean \pm SD BLI signal one week postimplantation in the SHP-77 model or randomized on Day 3 postimplantation in the DMS273-DLL3 model. CAR T cells were injected intravenously (9×10^6 CAR⁺ cells/mouse in the SHP-77 model or 5×10^6 CAR⁺ cells/mouse in the DMS273-DLL3 model). In both models, tumors continued to be monitored every 3 to 4 days after CAR T infusion using BLI system until the end of the study. In both subcutaneous and systemic models, the group sizes were calculated on the basis of similar historical study data and experience.

Mouse safety study using animals bearing subcutaneous tumor

Prior to tumor implantation, adeno-associated viruses (AAV) encoding IL7 & IL15 (Vigene Biosciences) were injected in NSG mice through tail vein intravenously to support CAR T-cell expansion and persistence. LN229-mDLL3 cells (4.25×10^6 per mouse) were injected in 200 μ L subcutaneously 1:1 with Matrigel Membrane Matrix (Corning 354234) in NSG mice. Tumor growth was monitored by caliper measurements and tumor size was calculated as described above. Three weeks postimplantation, mice were assigned to groups such that each group had similar mean \pm SD tumor volume and serum

concentration of IL7 and IL15. CAR T cells were injected intravenously (1×10^7 CAR⁺ cells/mouse). Tumors continued to be monitored every 3 to 4 days until the end of the study. Serum was collected for cytokine analysis using MSD. On day 49, brain and pituitary tissues from animals were fixed in 10% NBF and stained with H&E or anti-CD3 antibody (Abcam, clone EP449E). The H&E slides were examined microscopically and histopathologic findings were scored by a pathologist using a standard system.

***In vitro* cytotoxicity of disassociated mouse pituitary cells**

Mouse pituitaries from NSG mice were harvested under aseptic conditions for *in vitro* analysis, as described in Supplementary Materials and Methods. Cells were plated in 96-well plate and let to recover for 3 days before CAR Ts were added. For controls, DLL3⁺ cells (DMS-273) and DLL3⁻ cells (293T) were plated at the same densities. Short-term cytotoxicity assay was performed as described above with the exception that CellTiter Glo (Promega) was utilized. At the end of 3 day co-culture, the T cells were pooled and stained for activation markers (41BB and CD25) for analysis by flow cytometry. The supernatant was harvested for cytokine analysis using Human TH1/TH2 10-Plex Tissue Culture Kit (Meso Scale Discovery, K15010B) following manufacturer's protocol.

Statistical methods

All statistical analyses were performed with GraphPad Prism software. Statistical methods used for each experiment are described in the figure legend. When applicable, groups were pruned to the latest time point before any animal in the group reached endpoint. Imaging data were log-transformed prior to analysis.

Data availability

All data associated with this study are presented in the paper or Supplementary Materials and Methods. Raw data generated in this study are available upon reasonable request from the corresponding authors.

Results

DLL3 expression on SCLC cell lines, tumors, and normal tissues

In evaluating potential cell surface targets for SCLC CAR T therapy, we sought to identify antigens with high expression on SCLC tumor cells and limited expression on essential normal tissues. Using published primary SCLC RNA-seq data (17) and the Cancer Cell Line Encyclopedia (CCLE), we evaluated *DLL3* RNA expression in 55 primary tumors and 47 SCLC cell lines. *DLL3* mRNA was highly expressed in SCLC primary tumors and at similar levels in SCLC cell lines (Supplementary Fig. S1A). RNA-seq results from the Genotype-Tissue Expression (GTEx) database of primary normal (nonmalignant) tissue types demonstrate that *DLL3* is not expressed in the majority of normal tissues although some *DLL3* mRNA is detected in the pituitary gland, brain, and testis (Supplementary Fig. S1B). To confirm these results, RNA *in situ* hybridization (ISH) was used to further examine *DLL3* expression on SCLC tumors, SCLC cell lines, and a large panel of normal tissues from up to three donors and expression was given a semiquantitative visual score (RNAscope score) of 0 to 4. Our results demonstrated *DLL3* RNA expression in most of the SCLC tumors and both SCLC cell lines tested. *DLL3* expression was detected in two of three normal pituitary glands, confirming the data from GTEx (Supplementary Figs. S1C and S1D). We next explored *DLL3* expression on the surface of SCLC cell lines and disassociated PDX tumors using flow cytometry. Five SCLC cell lines covering the

range of *DLL3* RNA expression of most SCLC tumors (Supplementary Fig. S1A) and one melanoma cell line WM266-4 were selected for the analysis and *DLL3* protein expression on the cell surface ranged from ~500 copies to ~3,500 copies per cell. The expression on five representative SCLC PDX models was similar to that of SCLC cell lines (Supplementary Fig. S1E).

Generation and characterization of *DLL3* antibodies

Anti-*DLL3* antibodies were generated in multiple hybridoma campaigns, with recombinant human *DLL3* used as an immunogen. To avoid host anti-murine CAR immune responses in patients, transgenic animals that express functional human Ig genes were used for hybridoma development. Anti-*DLL3* antibodies were screened against *DLL3*

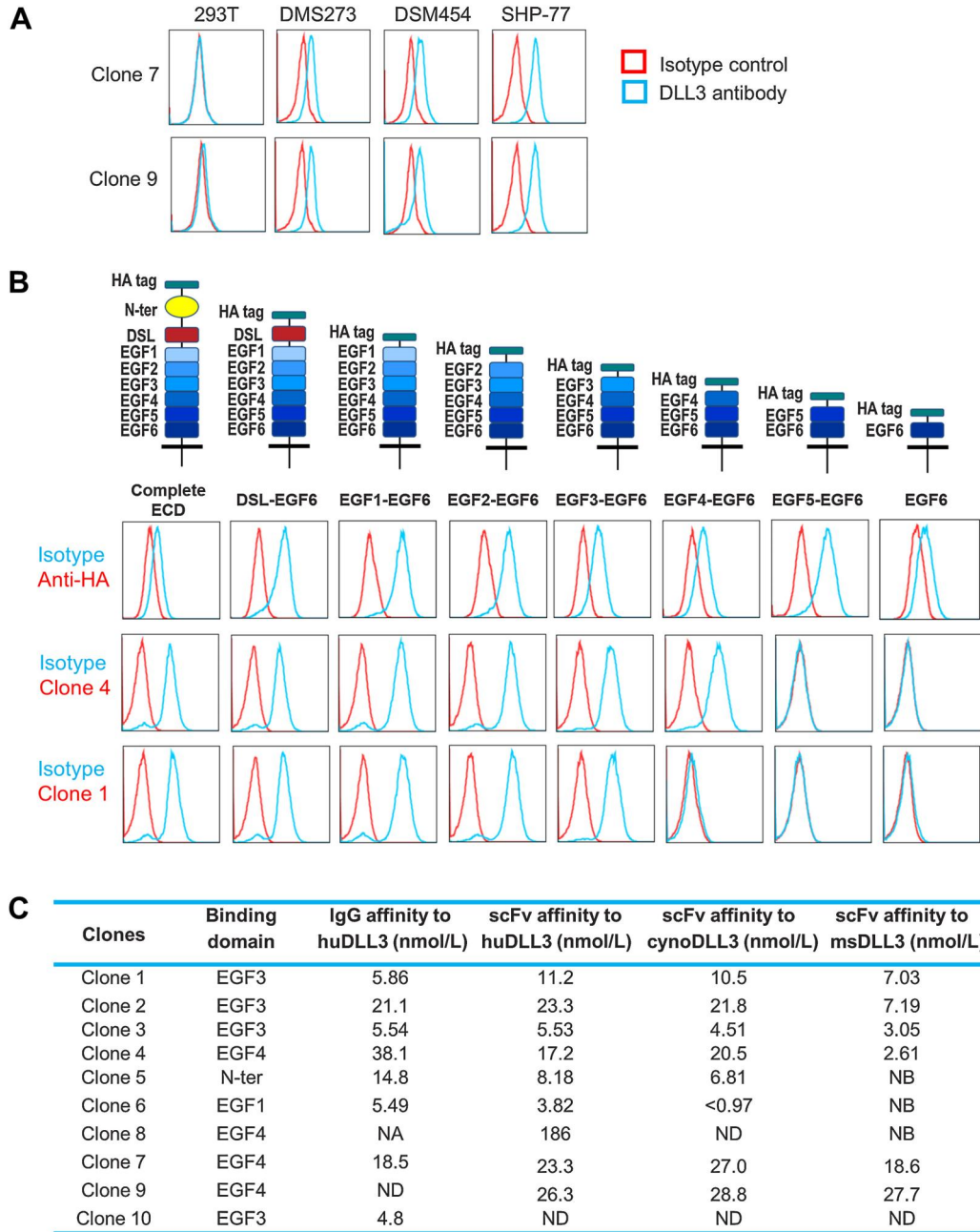


Figure 1.

DLL3 antibodies were generated and characterized *in vitro* to determine binding epitopes and kinetics. **A**, Flow cytometry analysis demonstrating two representative *DLL3* clones bind to *DLL3*-positive DMS273, WM266-4, and SHP-77 cells but not *DLL3*-negative 293T cells. **B**, Schematic representation of full-length and truncated human *DLL3* proteins expressed on CHO cells for epitope mapping. All constructs contained an N-terminal HA tag for easy detection. Epitope mapping of two *DLL3* antibodies recognizing EGF3 and EGF4 domain are shown. **C**, Affinity of anti-*DLL3* antibodies (either in full-length IgG format or scFv format) to human, cynomolgus monkey, and mouse *DLL3* proteins. Second column shows which extracellular domain of human *DLL3* each of anti-*DLL3* antibodies recognizes. NB, no binding; ND, not determined.

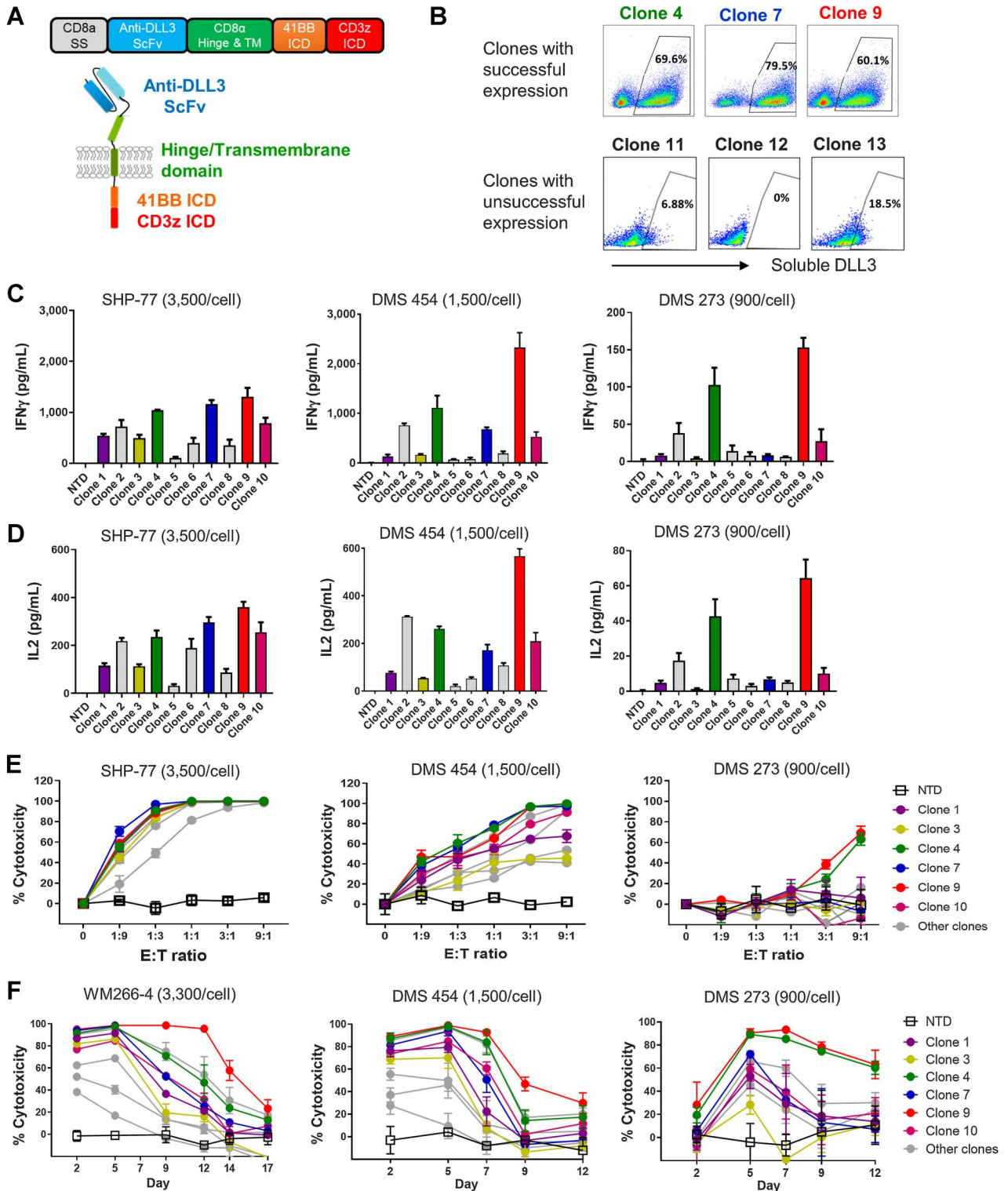


Figure 2. DLL3 CAR Ts are active against DLL3-positive cell lines. **A**, Schematic of a construct encoding an anti-DLL3 CAR. From the N-terminus to the C-terminus, the anti-DLL3 CAR includes anti-DLL3 scFv, the hinge and transmembrane regions of the CD8 α molecule, the cytoplasmic region of the 4-1BB molecule, and the cytoplasmic region of the CD3 ζ molecule. **B**, DLL3 clones were selected on the basis of appropriate cell surface expression. The plots are gated on live CD3⁺ cells. The numbers on the plots are the percentage of cells expressing each anti-DLL3 CAR. (Continued on the following page.)

using ELISA, followed by flow cytometry screening to determine binding to DLL3 negative and positive cell lines (Fig. 1A). The specificity for DLL3, and not related Notch ligands DLL1, DLL4, Jagged-1, or Jagged-4, was demonstrated by ELISA and the antibodies specific for DLL3 were selected for further evaluation.

To determine the binding epitope of the antibodies, a panel of CHO cells expressing full length or truncated human DLL3 variants was established. Specifically, the sequences of the respective eight extracellular domains (N-terminus, DSL, EGF1, EGF2, EGF3, EGF4, EGF5, and EGF6) of human DLL3 were deleted one by one, starting from the N-terminus (Fig. 1B). Each DLL3 antibody was tested for binding to this panel of cells and results demonstrated diverse epitope binding; all extracellular domains of DLL3 except EGF6 were bound by at least one antibody. Flow cytometry data of two representative antibodies are shown in Fig. 1B. Further, DLL3 antibodies with cross-reactivity to human, cynomolgus (cyno), and mouse DLL3 were identified using CHO cells expressing human, cyno, or mouse DLL3 and affinities determined by surface plasmon resonance (SPR) analysis with recombinant DLL3 for each species. Binding domains and affinity of 10 representative antibodies are summarized in Fig. 1C

Overall, multiple DLL3-specific antibodies with affinity in the nanomolar range were generated. Many antibodies had cross-reactivity to the mouse antigen, making them suitable for both efficacy and toxicity studies.

***In vitro* characterization of DLL3 CAR T cells**

Greater than 50 DLL3 antibodies were formatted into second-generation CARs with a CD8 signal sequence, CD8 hinge, and transmembrane domain, 4-1BB costimulatory domain, and CD3 ζ intracellular domain (Fig. 2A) and transduced into primary T cells using lentiviral vectors. CAR transduction efficiencies typically ranged from 20% to 80% and only clones that showed 30% transduction efficiency or greater, as detected by soluble DLL3, were selected for further development. Representative clones that showed successful (30% or greater) or unsuccessful (lower than 30%) cell surface expression are shown in Fig. 2B.

To evaluate the function of DLL3 CARs, CAR T cells were co-cultured with target cells spanning a range of DLL3 expression density. After a 24-hour coculture, DLL3 CAR T cells secreted multiple cytokines including IFN γ , TNF α , GM-CSF, and IL2. IFN γ and IL2 secretion from 10 representative clones are shown in Fig. 2C and D. For most of the clones, DLL3-high/med density cell lines SHP-77 (3,500/cell) and DMS 454 (1,500/cell) induced much higher cytokine secretion than DLL3-low density cell line DMS 273 (900/cell), suggesting DLL3 expression is a driver for CAR T effector function. After 3-day co-culture, DLL3 CAR T cells efficiently induced cytotoxicity in DLL3 positive cell lines across a broad range of effector-to-target cell (E:T) ratios. In general, greater cytotoxicity was seen in DLL3-high/med density cell lines SHP-77 and DMS 454 compared with DLL3-low DMS 273 cell line. At an E:T ratio of 1:1, almost all the clones induced complete cytotoxicity of SHP-77, but only ~30% to 80% cytotoxicity in DMS 454 and very limited cytotoxicity in DMS 273 (Fig. 2E), again suggesting that DLL3 density is a driver for CAR T-induced cytotoxicity.

Specificity of DLL3 CARs was verified by lack of cytotoxicity against DLL3 negative cells (Supplementary Figs. S2A and S2B). All the CARs that showed cytotoxicity in the 3-day assay were further evaluated in a long-term serial-killing assay to assess CAR function upon repeated target cell exposure (Fig. 2F). All CARs were able to kill target cells initially, but many lost activity after multiple re-challenges. WM266-4 cells was substituted for SHP77 in the long-term and Incucyte assays due to their more adherent properties. The six best performing CARs in the assay (shown in color) were selected for further evaluation.

Identification of optimal rituximab-based off-switch formats for lead DLL3 CARs

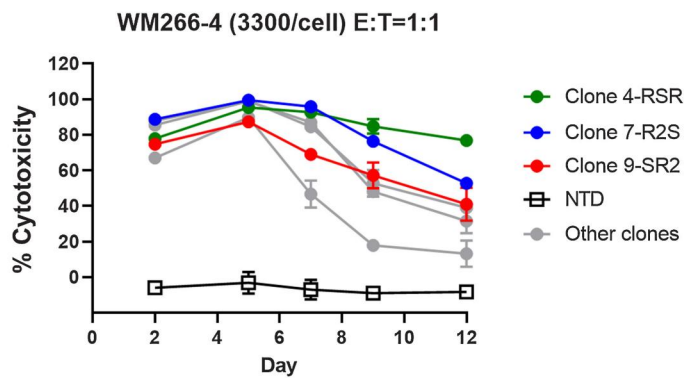
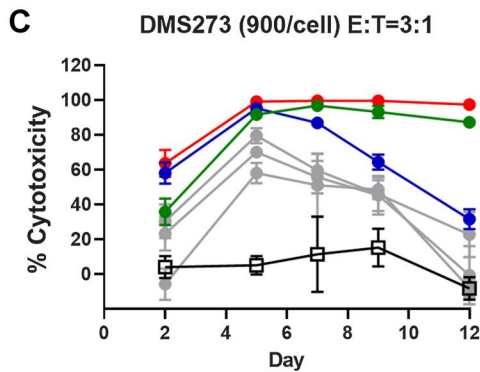
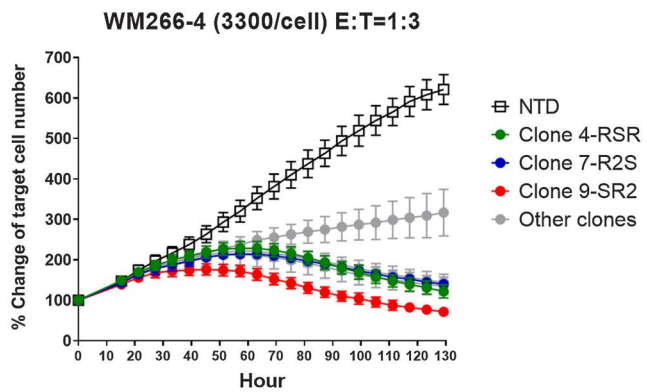
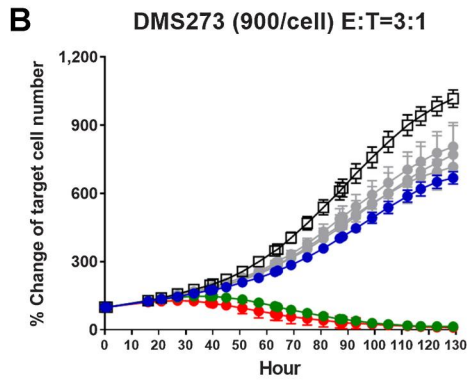
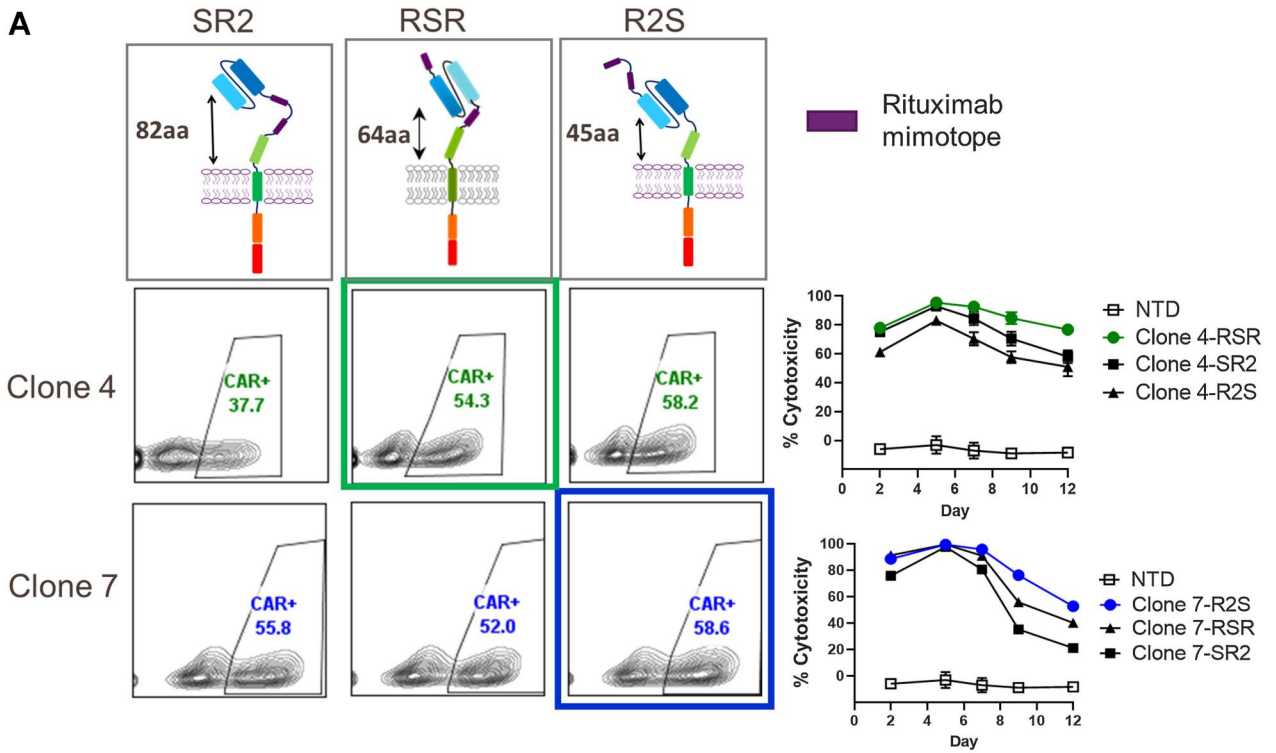
CAR T-cell therapies have the potential for on-target and off-tumor toxicities to normal tissues, so a CAR off-switch may be desired to eliminate CAR T cells in the case of unexpected adverse activity or in the context of cytokine release syndrome (CRS). A rituximab-based off-switch system was chosen using a rituximab mimotope, as rituximab is an FDA-approved mAb targeting CD20. Rituximab mimotopes have been previously incorporated into CARs and shown to modulate activity effectively (32–34). To identify an optimal safeguard CAR architecture, we assembled three different off-switch formats, each containing two CD20 mimotopes at different positions in the extracellular portion of the CAR (Fig. 3A). The top six performing CARs from the long-term serial-killing studies (Fig. 2F) were converted into these off-switch formats and transduced into primary T cells. CAR transduction efficiencies typically ranged from 35% to 65% as determined by flow cytometry (Fig. 3A) and were efficiently co-stained with rituximab and soluble DLL3 (Supplementary Fig. S3A), demonstrating correct folding of the scFv and the off-switch. On the basis of both transduction efficiency and cytotoxicity, an optimal off-switch format was chosen for each clone. As examples, the RSR format was optimal for Clone 4 and the R2S format was optimal for Clone 7 (Fig. 3A), demonstrating that optimal off-switch format is not universal across all CARs. The top six clones, each in their optimal off-switch format, were then evaluated in the short-term and long-term cytotoxicity assays with DMS 273 or WM266-4 target cells to identify the three lead candidates, clone 4-RSR, clone 7-R2S, and clone 9-SR2 (Fig. 3B and C).

To test the functionality of the off-switch, DLL3 CAR T cells were cultured with activated NK cells and rituximab, and their viability was measured by flow cytometry. Significant depletion of CAR T cells was observed upon incubation with both rituximab and NK cells relative to either rituximab or NK cells alone (Supplementary Fig. S3B), demonstrating that rituximab can mediate depletion of CAR T cells via antibody-dependent cell-mediated cytotoxicity (ADCC).

Antitumor efficacy in SCLC subcutaneous and systemic models

To evaluate the activity of DLL3 CAR T cells *in vivo*, SHP-77 cells were implanted subcutaneously in nonobese diabetic SCID γ (NSG) mice and allowed to engraft for 14 days before treatment with a single tail vein injection of 5×10^6 CAR T cells. All three lead clones, clone

(Continued.) C and D, DLL3 CAR Ts secrete IFN γ and IL2 when co-cultured with DLL3-positive cell lines with low (DMS 273), medium (DMS 454), and high (SHP-77) antigen density. CAR Ts and tumor cells were co-cultured for 24 hours at the E:T ratio of 1:1. E, Short-term cytotoxicity assay demonstrating that only a limited number of clones are capable of eliminating cells with a low density of cell surface. DLL3 CARs were co-cultured with luciferase-labeled target cell lines for 72 hours, and cell viability was analyzed in ONE-Glo assay. F, Superior clones from short-term killing also performed better in long-term killing assays. DLL3 CARs were evaluated in a long-term serial killing assay where CAR T cells were transferred to freshly plated target cells every 2 to 3 days. CARs that were highly active (shown in color) in both cytotoxicity assays are currently being investigated *in vivo*. In C–F, results represent mean \pm SD, $n = 3$. NT, nontransduced T cells. Numbers in the parentheses indicate surface copy number of DLL3.



4-RSR, clone 9-SR2, and clone 7-R2S, completely cleared the tumors (Fig. 4A). To understand durability of response, mice were followed out to day 87. The majority of mice remained tumor free, even after rechallenge with new tumor on day 69 (Supplementary Figs. S4A and S4B). To further differentiate these clones, a more challenging subcutaneous model with DMS 273 cells expressing exogenous DLL3 (DMS273-DLL3) was used. In this model, a single dose of 1×10^7 CAR T cells led to significant tumor inhibition and improved survival. Animals treated with clone 7-R2S had tumor outgrowth earlier than animals treated with clone 9-SR2 or clone 4-RSR. At 45 days after tumor implant, only mice treated with clone 4-RSR maintained 100% survival (Fig. 4B; Supplementary Fig. S4C). Effectiveness of the rituximab off-switch was also verified utilizing this model in a study where administration of rituximab was able to abolish anti-tumor effects of CAR T cells when administered to mice (Supplementary Fig. S4D).

To mimic the metastatic disease typically seen in patients with extensive stage SCLC, we established two systemic models with DMS273-DLL3 cells or SHP-77 cells. In the DMS273-DLL3 systemic model, tumor cells labeled with firefly luciferase were implanted via tail vein injection and formed large solid tumors in the liver, with small tumors also frequently detected in the lung and kidney (Supplementary Fig. S4E). Tumor bearing animals received a single dose of 5×10^6 CAR T cells and tumor burden was monitored by BLI. All three lead clones significantly delayed tumor growth and animals treated with clone 4-RSR had the lowest average tumor burden (Fig. 4C). At the end of the study, 5 of 8 animals treated with clone 4-RSR were tumor free whereas none of the animals treated with clone 7-R2S or clone 9-SR2 were tumor free (Supplementary Figs. S4F and S4G). In an SHP-77 systemic model, tumor cells implanted via tail vein injection were detected in multiple organs including lung, liver, kidney, and brain (Supplementary Fig. S4H). At the time of CAR T dosing, most of the tumor cells were concentrated in the lung with animals showing the brightest signal in the chest area. DLL3 CAR T cells quickly controlled tumor growth, with clone 4-RSR demonstrating more potent anti-tumor activity at the end of the study (Fig. 4D). At the end of the study, 3 of 8 animals treated with clone 4-RSR were tumor free whereas none of the animals treated with clone 7-R2S were tumor free (Supplementary Fig. S4I). Clone 9 was excluded from the study based on off-target binding analysis (discussed below). Treatment with both clones led to similar CAR T expansion (Fig. 4E), although clone 4-RSR produced higher levels of IFN γ and GM-CSF in mouse serum (Fig. 4F). Taken together, these data support that clone 4-RSR has the overall greatest anti-tumor activity in SCLC tumor models and is the potential lead candidate from an efficacy perspective.

Examination of lead DLL3 CARs for off-target binding

Antibodies or CARs can bind to not only their intended target but also to other proteins (off-target binding). To verify the specificity of DLL3 clones, in addition to specificity screening carried out during

antibody development (Fig. 1A), we further screened DLL3 CARs using a panel of DLL3-negative cell lines in cytotoxicity assays with no cytotoxic activity observed.

A tissue cross-reactivity (TCR) assay was also performed in which the binding domains from clone 4, 7, and 9 were generated in soluble form and screened for binding against a panel of 36 normal tissues from 1 human donor by IHC. Clone 9 stained the membrane of reticular cells and fibers as well as mononuclear cells in several tissues (Supplementary Fig. S5A). Also, clone 9 displayed cytoplasmic staining in more than 30 tissues. Given the nonspecific staining observed in almost all tissues with clone 9, it was de-prioritized. Clones 4 and 7 were further evaluated in a TCR study in compliance with Good Laboratory Practice (GLP) to evaluate the same panel of 36 normal tissues from 3 human donors. Clone 7 showed cytoplasmic staining of epithelial cells in the pituitary (adenohypophysis), skin (stratum corneum), and stromal cells in the ovary. Given that staining was not widespread and intracellular protein is not accessible to CAR T cells, staining of clone 7 was deemed acceptable. Clone 4 showed membrane staining in pancreatic epithelium and amnion in the placenta in all three donors as well as spermatogenic cells in the testis in one donor (Supplementary Fig. S5B). Membrane staining in pancreas (acinar and duct cells) was of the greatest concern due to the possibility of pancreatitis. This staining was not detected in the first TCR, even though the donor from the first TCR was also included in the GLP TCR, indicating that some methodological difference may be present between the two studies.

To resolve the conflict between the two TCR studies, a follow-up study was conducted with pancreas tissues from eight additional human donors and two independent preparations of soluble binding domain from clone 4. In contrast to the previous result, no membrane binding was observed with clone 4 in any of the eight human pancreas samples examined with either batch of reagent (Supplementary Fig. S5C). Additional IHC analysis performed using clone 4 soluble domain also did not detect membrane staining in 20 normal pancreas samples (Supplementary Figs. S5D and S5E). To support the staining results, additional experiments were performed to determine the potential of targeting pancreatic tissue with clone 4. Normal pancreas samples from three human donors were dissociated to generate single cell suspension and evaluated by flow cytometry. Clone 4 showed binding to the DLL3-positive DMS273 cells but not primary pancreatic cells (Supplementary Fig. S5F). Pancreatic cells were also co-cultured with DLL3 CAR T cells for 48 hours and evaluated for CAR T activation (4-1BB and CD25 expression). No signs of T-cell activation were observed (Supplementary Fig. S5G). Consistent with this, mouse DLL3 cross-reactive clone 4 CAR T cells showed only sparse infiltration into mouse pancreas and only minimal to mild decrease in zymogen granules, particularly in tele-insular regions away from the pancreatic islets (Supplementary Fig. S5H). This change was not associated with degeneration, increased apoptosis, or other acinar cell changes. Given the aggregate of the IHC data and the other pancreatic

Figure 3.

DLL3 CAR Ts with rituximab-based off-switch formats are active against DLL3-positive cells. **A**, Rituximab mimotopes (purple) were placed at different positions in the extracellular portion of the CAR. Numbers of amino acids between the transmembrane domain (TM) and scFv are shown and vary from 45 to 82. On the basis of both transduction efficiency and cytotoxicity, the RSR format was optimal for Clone 4 and the R2S format was optimal for Clone 7. Transduction efficiency was calculated as the percentage of cells that recognize soluble DLL3. Cytotoxicity was evaluated where CAR T cells were transferred to freshly plated target cells every 2 to 3 days. **B**, Top 6 clones in their optimal off-switch format were tested in incu-cyte-based short-term cytotoxicity assay. Nuclear GFP-labeled target cells were plated in a 96-well plate and counted every 6 hours. Three lead clones are shown in color. Results represent mean \pm SD, $n = 3$. **C**, Top 6 clones in their optimal off-switch format were tested in the long-term cytotoxicity assay. CAR T cells were exposed to new luciferase-labeled target cells every 2 to 3 days for a total of 12 days. ONE-Glo luminescence analysis was used to determine target cell viability. Three lead clones shown in color were selected for *in vivo* validation. Results represent mean \pm SD, $n = 3$.

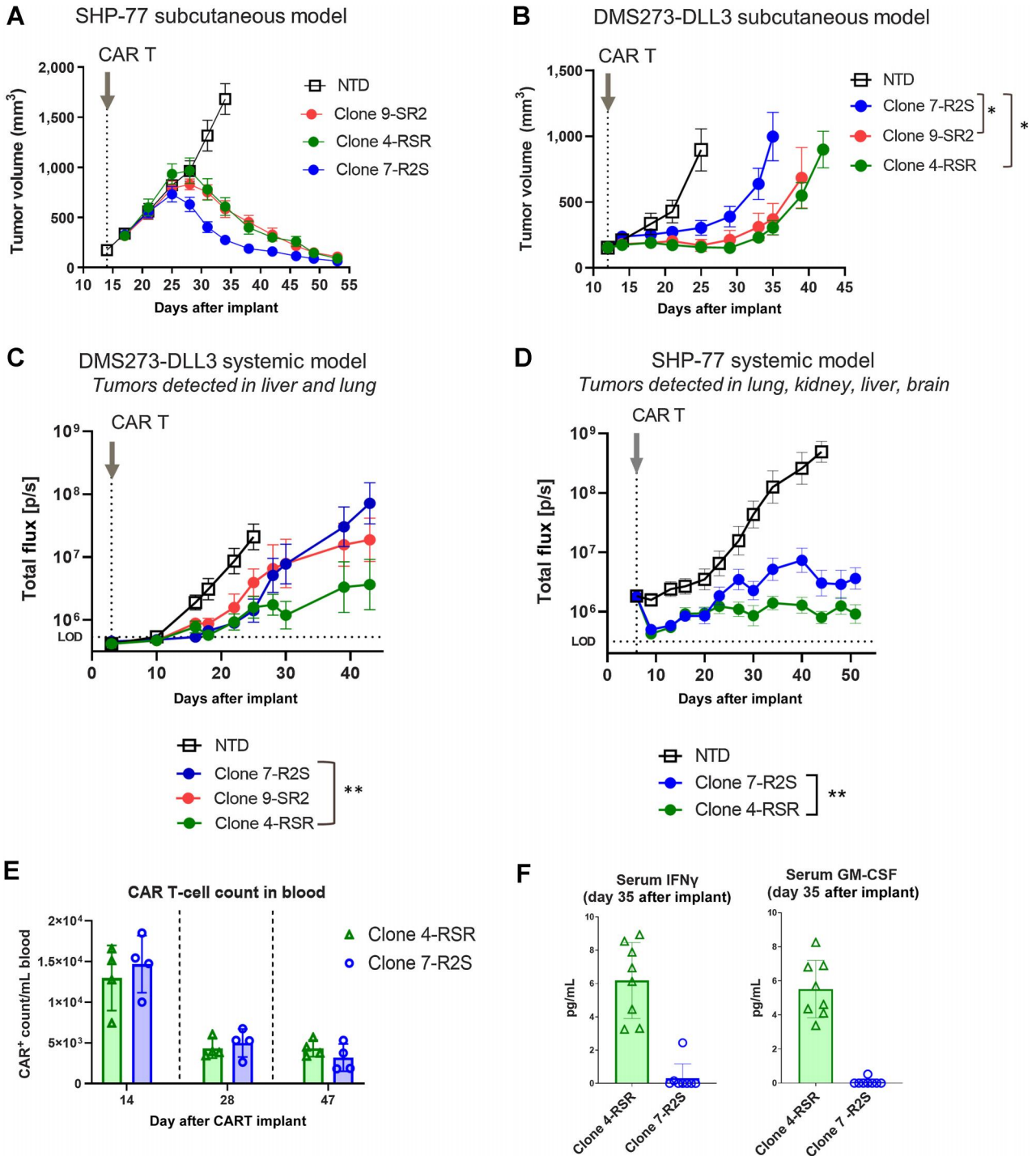


Figure 4. DLL3 CAR T cells are highly efficacious against established SCLC subcutaneous and systemic tumors. **A**, DLL3 CAR T cells induced complete regression of SHP-77 subcutaneous tumors. Tumors were established by injecting 5×10^6 SHP-77 cells subcutaneously. On day 14 after tumor implant, 5×10^6 CAR⁺ cells were given to animals by intravenous tail vein injection. Data represent mean \pm SEM. **B**, DLL3 CAR T cells substantially delayed progression of DMS273-DLL3 subcutaneous tumors. 1×10^5 DMS273-DLL3 cells were injected into the mouse flank. On day 12 after tumor implant, 1×10^7 CAR⁺ cells were given to animals by intravenous tail vein injection. Tumor measurements (day 12-35) were analyzed by RM one-way ANOVA with Tukey correction for multiple comparisons. Data represent mean \pm SEM (*, $P < 0.05$, $n = 8$). **C**, Luciferase-labeled DMS273-DLL3 cells (1×10^5 per animal) were inoculated intravenously. CAR Ts were dosed on day 3 after tumor implantation at 5×10^6 CAR⁺ cells per animal. Bioluminescent imaging was used to measure tumor volume. Statistical analysis was done using RM one-way ANOVA on D10-43 with Tukey multiple comparison test (*, $P < 0.05$, $n = 8-9$). Data represent mean \pm SEM. (Continued on the following page.)

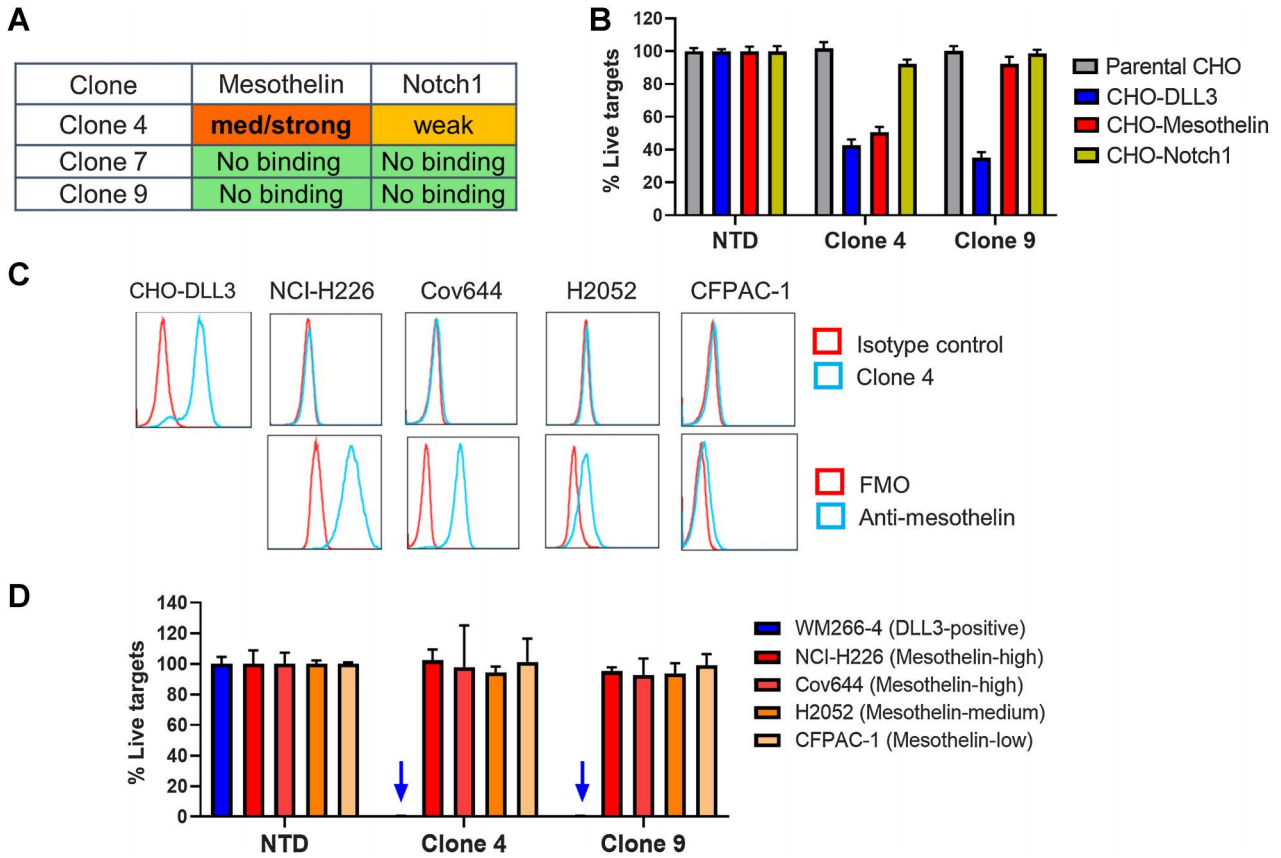


Figure 5.

Cell microarray-based binding assay to identify potential off-target binders of DLL3 CAR T clones. **A**, Binding of clones 4, 7, and 9 to potential off-target proteins was tested in a cell microarray screen of >5,000 transmembrane proteins. Clone 4 showed medium-to-strong binding of mesothelin and weak interaction to Notch1. No off-target proteins were identified for clone 7 or 9. **B**, CHO cells expressing DLL3, mesothelin, or Notch1 were established by lentivirus transduction and co-cultured with DLL3 CAR cells for 3 days at E:T ratio of 6:1. Clone 4 showed cytotoxicity against DLL3 or mesothelin-expressing CHO cells but not Notch1-expressing CHO cells. **C**, Clone 4 showed binding to CHO-DLL3 cells but not four cell lines (NCI-H226, Cov644, H2052, and CFPAC-1) that express endogenous mesothelin. **D**, Clones 4 and 9 showed cytotoxicity against DLL3-positive WM266-4 cells but not the four endogenous mesothelin-expressing cell lines shown in **C**. All target cells were co-cultured with DLL3 CAR T cells for 3 days at an E:T ratio of 6:1. Arrows represent conditions with a value of zero and no bar visible. In **B** and **D**, results represent mean \pm SD, $n = 3$ technical repeats. Experiments were performed twice with CAR T cells from two different donors.

derisking studies, we have concluded that the pancreatic staining may have been artifactual.

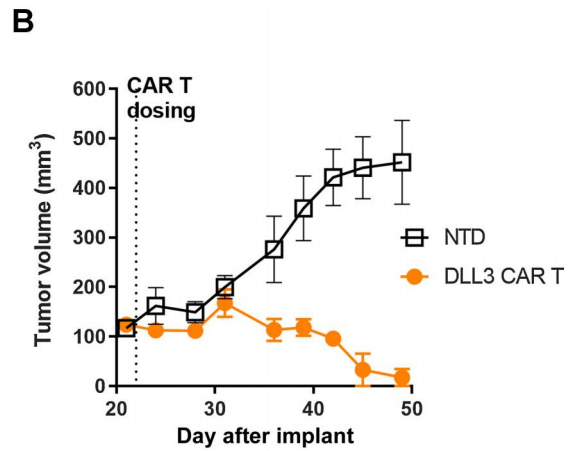
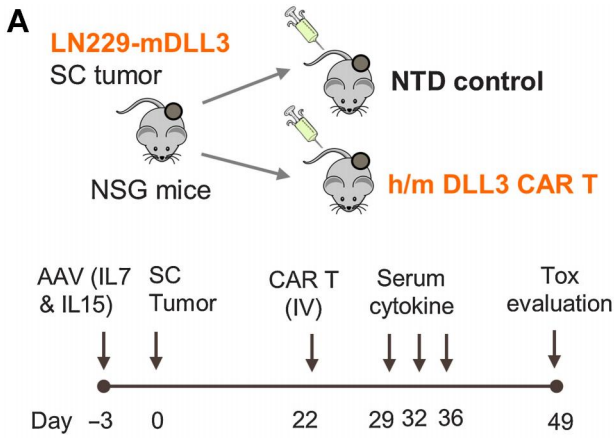
Given the inconsistencies between the three TCR studies, an orthogonal assay was chosen to assess off-target binding. A Retrogenix assay was chosen, in which protein-protein interactions are tested with HEK293 cells arrayed to overexpress more than 5,000 human plasma membrane proteins (35). This assay utilizes minimally fixed cells. DLL3 clones in full length IgG format were generated and assessed for binding by automated fluorescent microscopy. No off-target binders were identified for clone 7 whereas clone 4 showed medium-to-strong binding to mesothelin and weak binding to Notch 1 (Fig. 5A). Co-culture of clone 4 CAR Ts with CHO cells overexpressing Notch 1 did not result in cytotoxicity even at a high E:T ratio of 6:1 (Fig. 5B),

suggesting this interaction is too weak or the epitope is not correctly orientated to trigger T-cell effector function. In addition, although clone 4 lysed CHO cells overexpressing mesothelin (Fig. 5B), it did not bind to or lyse four cell lines expressing endogenous levels of mesothelin (Fig. 5C and D), suggesting the interaction with mesothelin might require supra-physiologic expression. Taken together these data demonstrate an acceptable safety profile for clone 4 and 7.

Mouse safety studies to understand potential toxicity liabilities in brain and pituitary

Human *DLL3* RNA is expressed in normal pituitary and brain tissues (Supplementary Figs. S1B and S1C). Mouse *Dll3* RNA is also expressed in pituitary (Bio-GPS) and brain (Supplementary Fig. S6A),

(Continued.) **D**, Luciferase-labeled SHP-77 cells were inoculated intravenously and infiltrated into multiple tissues. CAR Ts were dosed at 9×10^6 CAR⁺ cells per animal on day 7 after implant. Bioluminescent imaging was used to measure tumor volume twice weekly. Tumor measurements (day 2-44) were analyzed by using paired *t* test (**, $P < 0.01$, $n = 8$). Data represent mean \pm SEM. **E**, Animals treated with clone 4-R2S and clone 7-RSR showed similar CAR T-cell count in the blood. Whole blood from animals was collected on days 14, 28, and 47 after tumor implant and stained with anti-human CD45 and recombinant DLL3 to detect CAR T cells. Error bars represent SD. **F**, Animals treated with clone 4-RSR showed higher levels of IFN γ and GM-CSF. Serum was collected on day 28 after CAR T infusion. Cytokines were measured using human proinflammatory tissue culture 9-plex assay (MSD) following manufacturer's protocol. Results represent mean \pm SD, $n = 8$.



C Human CD3 staining (day 49)

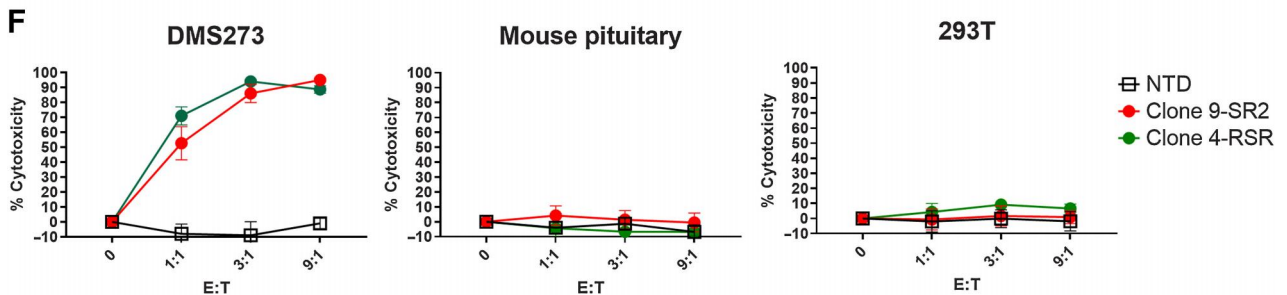
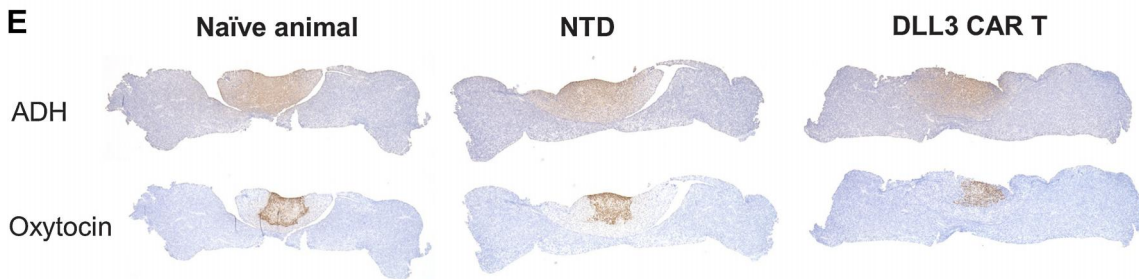
Group	Animal	Brain	Pituitary
NTD	#3	1	1
	#4	1	1
	#5	1	1
DLL3 CAR T	#1	2	3 (pars intermedia and nervosa)
	#2	1	3 (pars intermedia and nervosa)
	#3	1	3 (pars intermedia and nervosa)

Staining score:
 0 = No staining;
 1 = Sparse-to-moderately low staining;
 2 = Moderate-to-moderately high staining;
 3 = Abundant staining

D Histopathology analysis (day 49)

Group	Animal	Brain	Pituitary
NTD	#3	No lesions	No lesions
	#4	No lesions	No lesions
	#5	No lesions	No lesions
DLL3 CAR T	#1	No lesions	Infiltrate, mixed cell (severity=3)
	#2	No lesions	Infiltrate, mononuclear cell(severity=2)
	#3	No lesions	Infiltrate, mononuclear cell(severity=2)

**Severity: 1=Minimal; 2=Mild; 3=Moderate



suggesting mice are relevant toxicity models. To understand the potential toxicity liabilities of this normal tissue RNA expression, nontransduced (NTD) T cells or DLL3 CAR T cells were intravenously injected into NSG mice. One, two, or four weeks after injection, spleens, brains, and pituitaries were harvested and stained with human-specific CD3 (hCD3) antibody to detect human T cells by IHC. Although a small number of T cells were found in spleens from all animals, they were rarely detected in brain or pituitary samples (Supplementary Fig. S6B).

Even though no toxicity was observed in the nontumor bearing mouse model, toxicity may be underestimated in the absence of CAR T activation or target-driven expansion. To replicate the conditions in a patient where CAR T cells are stimulated by DLL3-positive tumors and proliferate as a result, DLL3 CAR T cells were injected into NSG mice bearing subcutaneous LN229 tumors that express exogenous mouse DLL3 (LN229-mDLL3). Mice were also injected with adeno-associated viruses (AAV) encoding IL7 and IL15 to maximize CAR T engraftment and activity and therefore to provide the greatest possible chance to see on-target toxicity (Fig. 6A). After tumors were established, 1×10^7 mouse DLL3 cross-reactive CAR T cells or NTD T cells were intravenously injected into animals. Throughout the study, none of the animals showed significant loss of body weight (Supplementary Fig. S6C) or abnormal behavior. Serum was collected on days 29, 32, and 36 for cytokine analysis. IFN γ secretion suggested CAR T activity was generally highest on day 32 among the three timepoints (Supplementary Fig. S6D). When animals treated with DLL3 CAR T cells were tumor free at day 49 (Fig. 6B), brain tissues were fixed and stained with hCD3 to detect T cells and with hematoxylin and eosin (H&E) to examine morphology. Administration of DLL3 CAR T cells resulted in abundant hCD3-positive T cells in the pituitary pars intermedia and nervosa (hCD3 staining score = 3; Fig. 6C). Relatively low levels of T cells were present in brain neuropil and vasculature (as circulating T cells; hCD3 staining score = 1–2; Fig. 6C). No tissue damage was observed (Fig. 6D). To understand, the functional consequences of T-cell infiltration in pituitary, expression of two hormones released in the pars nervosa, vasopressin (ADH), and oxytocin, were evaluated using IHC. Both hormones were detected in animals that received NTD T cells or DLL3 CAR T cells, suggesting that hormone-secreting cells in this region were not ablated (Fig. 6E).

A second safety study with similar design was conducted to evaluate potential toxicities on day 32 posttumor implant when CAR T activity was likely the highest among the three timepoints tested in the previous study (Supplementary Figs. S6D and S6E). Administration of DLL3 CAR T cells resulted in abundant hCD3-positive T cells in the tumor with relatively few T cells in the brain and pituitary (Supplementary Fig. S6F). Vasopressin and oxytocin expression were comparable in NTD T cells- and DLL3 CAR T cells-treated animals (Supplementary Fig. S6G). Consistent with this finding, no DLL3 protein was detected on mouse pituitary cells using flow cytometry (Supplementary

Fig. S6H) or IHC (Supplementary Fig. S6I), suggesting the DLL3 expression is very low and under the detection limit of both methods.

To directly investigate whether the DLL3 CAR Ts are active against the pituitary, mouse pituitaries from NSG mice were harvested, dissociated to single cells, and co-cultured with NTD T cells or DLL3 CAR T cells (clone 9 and clone 4) for 3 days (Supplementary Fig. S6J). For controls, DLL3-positive DMS273 and DLL3-negative 293T cells were plated at the same densities. No signs of pituitary cell death (Fig. 6F), CAR T activation (Supplementary Fig. S6K), or cytokine release (Supplementary Fig. S6L) were present with either clone 9 or clone 4. These data suggested DLL3 CAR Ts were not cytotoxic against primary pituitary cells.

To promote T-cell infiltration into the brain and further understand potential brain toxicity, NSG mice were intracranially implanted with LN229 tumors that express exogenous mouse DLL3 and human EGFRvIII (LN229-mDLL3-vIII). When tumors were established, NTD T cells, mouse DLL3 cross-reactive CAR T cells, or EGFRvIII CAR T cells (positive control) were intravenously injected (Supplementary Fig. S7A). The use of EGFRvIII CAR T cells allows for assessment of potential inflammation or tissue damage caused by tumor lysis in the brain. Both DLL3 CAR T cells and EGFRvIII CAR T cells significantly reduced tumor burden with some animals tumor-free at the end of the study (Supplementary Fig. S7B), suggesting that DLL3 CAR T cells were highly active in this model. None of the animals showed abnormal behavior or significant loss of body weight (Supplementary Fig. S7C). On days 22 and 36, brain and pituitary tissues were harvested from 5 animals in each group per timepoint and stained with H&E or human-specific CD45 (hCD45) by IHC. The histopathologic findings from H&E and hCD45-stained slides were scored by a pathologist. Animals treated with EGFRvIII CAR T cells had higher levels of T-cell infiltration on day 22 than on day 36 in areas of infiltrate/gliosis or glioma, consistent with antitumor activity on day 22. No brain tissue damage beyond tumor growth was observed (Supplementary Fig. S7D). Animals that received DLL3 CAR T cells, on the other hand, had more T-cell infiltration associated with the small foci of glioma on day 36 than on day 22 (Supplementary Fig. S7E), consistent with antitumor activity in this group on day 36. These animals also had infiltrates in the pituitary gland on day 36 (Supplementary Fig. S7D), primarily in the pars intermedia and nervosa but the hormone-secreting function was not affected, consistent with experiments described earlier (Supplementary Fig. S7F). No tissue damage was observed in pituitary or brain.

Discussion

CAR T-cell therapies have shown impressive efficacy in multiple hematologic malignancies and could be transformative for SCLC. Analysis of protein expression by flow cytometry confirmed DLL3 protein expression on the cell surface of SCLC PDX models, consistent with a previous report (36). Previous IHC studies concluded DLL3 membrane expression was not only detected in

Figure 6.

Mouse safety study with subcutaneous tumor showed T-cell infiltration in pituitary of DLL3 CAR-treated animals but no tissue damage. **A** and **B**, Design and antitumor efficacy in subcutaneous tumor toxicity model. Tumors were established by injecting 4.25×10^6 LN229-mDLL3 cells subcutaneously. Three weeks after tumor implant, 1×10^7 CAR⁺ cells were given to animals by intravenous tail vein injection. Results represent mean \pm SEM, $n = 5$. **C**, Anti-human CD3 staining shows T-cell infiltration in pituitary of DLL3 CAR-treated animals. Stained brain and pituitary samples were scored by a board-certified pathologist. **D**, Histopathology analysis showed mild infiltration/inflammation in pituitary of DLL3 CAR-treated animals with no other findings. **E**, IHC staining of ADH and oxytocin in mouse pituitary samples suggest hormone secreting cells were not ablated. **F**, DLL3 CAR T cells are not cytotoxic against mouse pituitary cells. DLL3 CAR T cells were co-cultured with DLL3-positive DMS273 cells, primary mouse pituitary cells, or DLL3-negative 293T cells for 3 days. Cytotoxicity of target cells was measured with CellTiter-Glo. Results represent mean \pm SD, $n = 3$ technical replicates. Experiment was performed three times.

treatment naïve patients but also in recurrent and treatment-refractory patients (36, 37) who are more likely to be the target patient population for CAR T therapy. Besides SCLC, *DLL3* RNA and protein are also detected in several other types of neuroendocrine tumors (38–42), allowing potential application of DLL3 CAR T therapy in these tumor types.

Antigen density has emerged as an important factor influencing the activity of CAR T cells (43–47). Copy-number analysis revealed that all SCLC PDX models tested expressed lower than 2,000 copies of *DLL3* per cell. In light of this information, SCLC cell lines with low surface copy number (DMS 273 and DMS 454) were targeted for evaluation to more accurately reflect expression levels expected in patients. In the short-term and long-term cytotoxicity assay, DLL3 CAR T cells demonstrated potent and specific killing activity against targets, including high sensitivity for cells with low-antigen density (900/cell). These assays clearly separated out optimal CAR Ts, particularly when using cells with very low *DLL3* expression, enabling selection of CARs most likely to work against patient tumors with low expression.

To identify any potential off-target binding of the antibody moiety of the CAR T, tissue cross-reactivity studies was conducted. Although these studies have been regarded as a gold-standard for examining off-target binding, they rely on high protein concentrations which may cause artifactual binding. In addition, the use of fixed and processed tissues may allow binding that would not be present under more biologically relevant conditions (48). Given that binding to pancreatic epithelia was seen in one of these studies across all three samples tested, but was not seen in two other studies in any donors tested, the binding was ruled as artifactual. This conclusion is supported by the lack of pancreatic findings in a cyno *DLL3* bispecific study (49). Given the availability of more physiologic assays such as Retrogenix, and the advantages of being able to identify and interrogate any potential binding seen in these assays as demonstrated here, it seems likely that tissue cross-reactivity studies may be less relevant as part of the toxicologic assessment of therapeutics.

Thus far CAR T-cell therapy has shown limited success for the treatment of solid tumors. A major reason for this is that many solid tumor antigens (e.g., HER2 and CAIX) are also expressed in normal tissues and administration of CAR T cells targeting these antigens led to severe adverse events and sometimes death (50, 51). *DLL3* is a promising tumor antigen with the potential for minimal normal tissue toxicity. Previous work has demonstrated a favorable safety profile using T-cell redirecting protein therapeutics targeting *DLL3* (29, 49). CAR T cells may be even more potent than molecular T-cell redirection, thus requiring even more rigorous off-tumor toxicity assessment in preclinical models.

Because RNA for *DLL3* is detected in pituitary and brain, even in the absence of confirmation of protein expression, it is essential to understand the potential for on-target off-tumor toxicity. Mouse *DLL3* cross-reactive CAR T cells injected into nontumor-bearing mice were rarely detected in pituitary or brain up to 4 weeks after injection. In a model where CAR T cells were exposed to *DLL3*-positive tumors and supported by cytokines, tumor clearance and T-cell infiltration into pituitary were observed. This infiltration is likely not due to off-target binding of the *DLL3* clone used in mouse safety studies as we have observed the infiltration with multiple different *DLL3* clones. Consistent with our findings in mouse models, a study of *DLL3* BiTE in cynomolgus monkey model has also showed T-cell infiltration into pituitary (49), again suggesting *DLL3* expression in pituitary is the reason for T-cell infiltration. However, despite CAR T infiltration,

pituitary structure and function appeared normal and hormone secretion was detected. *Ex vivo* co-culture of pituitary cells and *DLL3* CAR T cells did not trigger T-cell effector function. It is possible that there are low levels of *DLL3* expressed on pituitary cells, but it is below the detection limit of our methods and below the antigen density threshold required to trigger CAR T cytotoxicity (52, 53).

Although protein therapeutics targeting *DLL3* dosed intravenously have shown no significant toxicity in published studies (27, 28), these molecules may have limited infiltration into the brain as compared with other tissues due to the blood–brain barrier and this may limit brain toxicity. To ensure that such limitations did not affect our assessment of *DLL3* CAR T safety, tumor cells were added to stimulate CAR T in the brain. CAR T infiltration and potent antitumor response was observed in the brain, but no tissue damage beyond tumor lysis was detected. We thus conclude that concerns related to targeting of normal brain or pituitary tissue via *DLL3* CAR T due to the observed *DLL3* RNA expression are largely mitigated.

In this study, an expansive set of *DLL3* CAR T clones were tested for activity. Top candidate *DLL3* CAR T cells induced potent and specific killing of SCLC cells *in vitro* and in SCLC mouse models with an acceptable safety profile. These data support the future clinical development of *DLL3* CAR T cells for the treatment of SCLC.

Authors' Disclosures

Y. Zhang reports a patent for US20210107979A1 pending as well as employment with Gilead Sciences Inc. S.K. Tacheva-Grigorova reports a patent for US20210107979A1 pending. J. Sutton reports personal fees from Allogene Therapeutics during the conduct of the study. T.J. Van Blarcom reports a patent for US20210107979A1 pending. B.J. Sasu reports a patent for US20210107979A1 pending. S.H. Panowski reports a patent for US20210107979A1 pending. No disclosures were reported by the other authors.

Authors' Contributions

Y. Zhang: Conceptualization, investigation, writing—original draft, writing—review and editing. **S.K. Tacheva-Grigorova:** Investigation, writing—original draft. **J. Sutton:** Investigation. **Z. Melton:** Investigation. **Y.S.L. Mak:** Investigation. **C. Lay:** Investigation. **B.A. Smith:** Investigation. **T. Sai:** Conceptualization, investigation. **T. Van Blarcom:** Investigation. **B.J. Sasu:** Conceptualization, writing—original draft, writing—review and editing. **S.H. Panowski:** Conceptualization, investigation, writing—original draft, writing—review and editing.

Acknowledgments

We thank the protein engineering department, the flow cytometry group, and the vivarium staff at Allogene Therapeutics, Inc., and Pfizer Inc., for their support. We thank Kevin Lindquist and his group for biosensor expertise and support. We thank Jessica Yu for her hybridoma expertise and support. The *DLL3* ALLO CAR-T program, which utilizes Collectis technology, is exclusively licensed from Collectis by Allogene, and Allogene holds global development and commercial rights. The TALEN gene-editing technology is pioneered and controlled by Collectis. All work was supported by Allogene Therapeutics.

The publication costs of this article were defrayed in part by the payment of publication fees. Therefore, and solely to indicate this fact, this article is hereby marked “advertisement” in accordance with 18 USC section 1734.

Note

Supplementary data for this article are available at Clinical Cancer Research Online (<http://clincancerres.aacrjournals.org/>).

Received July 27, 2022; revised September 29, 2022; accepted December 12, 2022; published first January 23, 2023.

References

1. Siegel RL, Miller KD, Fuchs HE, Jemal A. Cancer statistics, 2021. *CA Cancer J Clin* 2021;71:7–33.
2. Paz-Ares L, Dvorkin M, Chen Y, Reinmuth N, Hotta K, Trukhin D, et al. Durvalumab plus platinum–etoposide versus platinum–etoposide in first-line treatment of extensive-stage small-cell lung cancer (CASPIAN): a randomised, controlled, open-label, phase 3 trial. *Lancet North Am Ed* 2019;394:1929–39.
3. Horn L, Mansfield AS, Szczesna A, Havel L, Krzakowski M, Hochmair MJ, et al. First-line atezolizumab plus chemotherapy in extensive-stage small-cell lung cancer. *N Engl J Med* 2018;379:2220–9.
4. Rudin CM, Brambilla E, Faivre-Finn C, Sage J. Small-cell lung cancer. *Nat Rev Dis Primers* 2021;7:3.
5. Grupp SA, Kalos M, Barrett D, Aplenc R, Porter DL, Rheingold SR, et al. Chimeric antigen receptor-modified T cells for acute lymphoid leukemia. *N Engl J Med* 2013;368:1509–18.
6. Neelapu SS, Locke FL, Bartlett NL, Lekakis LJ, Miklos DB, Jacobson CA, et al. Axicabtagene ciloleucel CAR T-cell therapy in refractory large B-cell lymphoma. *N Engl J Med* 2017;377:2531–44.
7. Abramson JS, Palomba ML, Gordon LI, Lunning MA, Wang M, Arnason J, et al. Lisocabtagene maraleucel for patients with relapsed or refractory large B-cell lymphomas (TRANSCEND NHL 001): a multicentre seamless design study. *Lancet* 2020;396:839–52.
8. Munshi NC, Anderson LD, Shah N, Madduri D, Berdeja J, Lonial S, et al. Idecabtagene vicleucel in relapsed and refractory multiple myeloma. *N Engl J Med* 2021;384:705–16.
9. Berdeja JG, Madduri D, Usmani SZ, Jakubowiak A, Agha M, Cohen AD, et al. Ciltacabtagene autoleucel, a B-cell maturation antigen-directed chimeric antigen receptor T-cell therapy in patients with relapsed or refractory multiple myeloma (CARTITUDE-1): a phase 1b/2 open-label study. *Lancet North Am Ed* 2021;398:314–24.
10. Metelo AM, Jozwik A, Luong LA, Dominey-Foy D, Graham C, Attwood C, et al. Allogeneic Anti-BCMA CAR T cells are superior to multiple Myeloma-derived CAR T cells in preclinical studies and may be combined with gamma secretase Inhibitors. *Cancer Research Communications* 2022;2:158–71.
11. Fraietta JA, Lacey SF, Orlando EJ, Pruteanu-Malinici I, Gohil M, Lundh S, et al. Determinants of response and resistance to CD19 chimeric antigen receptor (CAR) T cell therapy of chronic lymphocytic leukemia. *Nat Med* 2018;24:563–71.
12. Chapman G, Sparrow DB, Kremmer E, Dunwoodie SL. Notch inhibition by the ligand DELTA-LIKE 3 defines the mechanism of abnormal vertebral segmentation in spondylocostal dysostosis. *Hum Mol Genet* 2011;20:905–16.
13. Kusumi K, Dunwoodie SL, Krumlauf R. Dynamic expression patterns of the pudgy/spondylocostal dysostosis gene *Dll3* in the developing nervous system. *Mech Dev* 2001;100:141–4.
14. Ladi E, Nichols JT, Ge W, Miyamoto A, Yao C, Yang LT, et al. The divergent DSL ligand *Dll3* does not activate Notch signaling but cell autonomously attenuates signaling induced by other DSL ligands. *J Cell Biol* 2005;170:983–92.
15. Geffers I, Serth K, Chapman G, Jaekel R, Schuster-Gossler K, Cordes R, et al. Divergent functions and distinct localization of the Notch ligands *DLL1* and *DLL3* in vivo. *J Cell Biol* 2007;178:465–76.
16. Kunnimalaiyaan M, Chen H. Tumor suppressor role of Notch-1 signaling in neuroendocrine tumors. *Oncologist* 2007;12:535–42.
17. George J, Lim JS, Jang SJ, Cun Y, Ozretia L, Kong G, et al. Comprehensive genomic profiles of small cell lung cancer. *Nature* 2015;524:47–53.
18. Lim JS, Ibaseta A, Fischer MM, Cancilla B, O'Young G, Cristea S, et al. Intratumoral heterogeneity generated by Notch signaling promotes small cell lung cancer. *Nature* 2017;545:360.
19. SL J, Ibaseta A, F marcus, Cancilla B, Cristea S, Luca VC, et al. Intratumoral heterogeneity generated by Notch signalling promotes small-cell lung cancer. *Nature* 2017;545:360–4.
20. Shue YT, Drains AP, Li NY, Pearsall SM, Morgan D, Sinnott-Armstrong N, et al. A conserved YAP/Notch/REST network controls the neuroendocrine cell fate in the lungs. *Nat Commun* 2022;13:2690.
21. Rudin CM, Pietanza MC, Bauer TM, Ready N, Morgensztern D, Glisson BS, et al. Rovalpituzumab tesirine, a DLL3-targeted antibody-drug conjugate, in recurrent small-cell lung cancer: a first-in-human, first-in-class, open-label, phase 1 study. *Lancet Oncol* 2017;18:42–51.
22. Morgensztern D, Besse B, Greillier L, Santana-Davila R, Ready N, Hann CL, et al. Efficacy and safety of rovalpituzumab tesirine in third-line and beyond patients with DLL3-expressing, relapsed/refractory small-cell lung cancer: results from the phase II TrINITY study. *Clin Cancer Res* 2019;25:6958–66.
23. Blackhall F, Jao K, Greillier L, Cho BC, Penkov K, Reguart N, et al. Efficacy and safety of rovalpituzumab tesirine compared with topotecan as Second-line therapy in DLL3-High SCLC: results from the phase 3 TAHOE Study. *J Thorac Oncol* 2021;16:1547–58.
24. Sharma S, Li Z, Bussing D, Shah DK. Evaluation of quantitative relationship between target expression and antibody-drug conjugate exposure inside cancer cells. *Drug Metab Dispos* 2020;48:368–77.
25. Malhotra J, Nikolinakos P, Leal T, Lehman J, Morgensztern D, Patel JD, et al. A Phase 1–2 study of rovalpituzumab tesirine in combination with nivolumab plus or minus ipilimumab in patients with previously treated Extensive-stage SCLC. *J Thorac Oncol* 2021;16:1559–69.
26. Johnson ML, Zvirbule Z, Laktionov K, Helland A, Cho BC, Gutierrez V, et al. Rovalpituzumab tesirine as a maintenance therapy after first-line platinum-based chemotherapy in patients with extensive-stage-SCLC: results from the phase 3 MERU study. *J Thorac Oncol* 2021;16:1570–81.
27. Hipp S, Voynov V, Drobits-Handl B, Giragossian C, Trapani F, Nixon AE, et al. A bispecific DLL3/CD3 IgG-like T-cell engaging antibody induces antitumor responses in small cell lung cancer. *Clin Cancer Res* 2020;26:5258–68.
28. Giffin MJ, Cooke K, Lobenhofer EK, Estrada J, Zhan J, Deegen P, et al. AMG 757, a half-life extended, DLL3-targeted bispecific T-cell engager, shows high potency and sensitivity in preclinical models of small-cell lung cancer. *Clin Cancer Res* 2021;27:1526–37.
29. Aaron WH, Austin R, Barath M, Callihan E, Cremin M, Evans T, et al. Abstract C033: HPN328: an anti-DLL3 T cell engager for treatment of small cell lung cancer. *Mol Cancer Ther* 2019;18:C033.
30. NCT05507593. Study of DLL3-CAR-NK cells in the treatment of extensive stage small cell lung cancer. <https://clinicaltrials.gov/ct2/show/NCT05507593?cond=DLL3&draw=1&rank=2>; 2022.
31. Liu M, Huang W, Guo Y, Zhou Y, Zhi C, Chen J, et al. CAR NK-92 cells targeting DLL3 kill effectively small cell lung cancer cells *in vitro* and *in vivo*. *J Leukoc Biol* 2022;112:901–11.
32. Valton J, Guyot V, Boldajipour B, Sommer C, Pertel T, Juillerat A, et al. A versatile safeguard for chimeric antigen receptor T-cell immunotherapies. *Sci Rep*. 2018;8:8972.
33. Sommer C, Cheng HY, Nguyen D, Dettling D, Yeung YA, Sutton J, et al. Allogeneic FLT3 CAR T cells with an Off-switch exhibit potent activity against AML and can be depleted to expedite bone marrow recovery. *Mol Ther* 2020;28:2237–51.
34. Sommer C, Boldajipour B, Kuo TC, Bentley T, Sutton J, Chen A, et al. Preclinical evaluation of allogeneic CAR T cells targeting BCMA for the treatment of multiple myeloma. *Mol Ther* 2019;27:1126–38.
35. Freeth J, Soden J. New advances in cell microarray technology to expand applications in target deconvolution and Off-target screening. *SLAS Discovery* 2020;25:223–30.
36. Saunders LR, Bankovich AJ, Anderson WC, Aujay MA, Bheddah S, Black KA, et al. A DLL3-targeted antibody-drug conjugate eradicates high-grade pulmonary neuroendocrine tumor-initiating cells *in vivo*. *Sci Transl Med* 2015;7:302ra136.
37. Kuempers C, Jagomast T, Krupar R, Paulsen FO, Heidel C, Ribbat-Idel J, et al. Delta-like protein 3 expression in paired chemo-naive and chemorelapsed small cell lung cancer samples. *Front Med* 2021;8:734901.
38. Koshkin VS, Garcia JA, Reynolds J, Elson P, Magi-Galluzzi C, McKenney JK, et al. Transcriptomic and protein analysis of small-cell bladder cancer (SCBC) identifies prognostic biomarkers and DLL3 as a relevant therapeutic target. *Clin Cancer Res* 2019;25:210–21.
39. Puca L, Gavyert K, Sailer V, Conteduca V, Dardenne E, Sigouros M, et al. Delta-like protein 3 expression and therapeutic targeting in neuroendocrine prostate cancer. *Sci Transl Med* 2019;11:eaav0891.
40. Spino M, Kurz SC, Chiriboga L, Serrano J, Zeck B, Sen N, et al. Cell surface notch ligand *dll3* is a therapeutic target in isocitrate dehydrogenase–mutant glioma. *Clin Cancer Res* 2019;25:1261–71.
41. Xie H, Kaye FJ, Isse K, Sun Y, Ramoth J, French DM, et al. Delta-like protein 3 expression and targeting in merkel cell carcinoma. *Oncologist* 2020;25:810–7.
42. Sano R, Krytska K, Tsang M, Erickson SW, Teicher BA, Saunders L, et al. Abstract LB-136: pediatric preclinical testing consortium evaluation of a DLL3-targeted antibody drug conjugate rovalpituzumab tesirine, in neuroblastoma. *Cancer Res* 2018;78:LB-136.

43. Walker AJ, Majzner RG, Zhang L, Wanhainen K, Long AH, Nguyen SM, et al. Tumor antigen and receptor densities regulate efficacy of a chimeric antigen receptor targeting anaplastic lymphoma kinase. *Mol Ther* 2017;25:2189–201.
44. Majzner RG, Theruvath JL, Nellan A, Heitzeneder S, Cui Y, Mount CW, et al. CAR T cells targeting B7-H3, a Pan-cancer antigen, demonstrate potent pre-clinical activity against pediatric solid tumors and brain tumors. *Clin Cancer Res* 2019;25:2560–74.
45. Watanabe K, Terakura S, Martens AC, van Meerten T, Uchiyama S, Imai M, et al. Target antigen density governs the efficacy of anti-CD20-CD28-CD3 ζ chimeric antigen receptor-modified effector CD8⁺ T cells. *J Immunol* 2015;194:911–20.
46. Caruso HG, Hurton LV, Najjar A, Rushworth D, Ang S, Olivares S, et al. Tuning sensitivity of CAR to EGFR density limits recognition of normal tissue while maintaining potent antitumor activity. *Cancer Res* 2015;75:3505–18.
47. Liu X, Jiang S, Fang C, Yang S, Olalere D, Pequignot EC, et al. Affinity-tuned ErbB2 or EGFR chimeric antigen receptor T cells exhibit an increased therapeutic index against tumors in mice. *Cancer Res* 2015;75:3596–607.
48. Paavilainen L, Edvinsson Å, Asplund A, Hober S, Kampf C, Pontén F, et al. The impact of tissue fixatives on morphology and antibody-based protein profiling in tissues and cells. *J Histochem Cytochem* 2010;58:237.
49. Lobenhofer E, Werner J, Giffin M, Engwall M, Davies R, Homann O, et al. P1.12–18 nonclinical safety assessment of AMG 757, a DLL3 Bispecific T cell engager, in the cynomolgus monkey. *J Thorac Oncol* 2019;14.
50. Morgan RA, Yang JC, Kitano M, Dudley ME, Laurencot CM, Rosenberg SA. Case report of a serious adverse event following the administration of T cells transduced with a chimeric antigen receptor recognizing ERBB2. *Mol Ther* 2010;18:843–51.
51. Lamers CHJ, Klaver Y, Gratama JW, Sleijfer S, Debets R. Treatment of metastatic renal cell carcinoma (mRCC) with CAIX CAR-engineered T-cells-a completed study overview. *Biochem Soc Trans* 2016;44:951–9.
52. Gudipati V, Rydzek J, Doel-Perez I, Gonçalves VDR, Scharf L, Königsberger S, et al. Inefficient CAR-proximal signaling blunts antigen sensitivity. *Nat Immunol* 2020;21:848–56.
53. Majzner RG, Rietberg SP, Sotillo E, Dong R, Vachharajani VT, Labanieh L, et al. Tuning the antigen density requirement for CAR T-cell activity. *Cancer Discov* 2020;10:702–23.